ARTICLE NO. 79-0435R

C80-060

Experiments with Omega Sensors for Measuring Stress in the Flexible Material of Parachute Canopies

00009
00032
30019

Gunter Braun* and Karl-Friedrich Doherr†
DFVLR—Institut für Flugmechanik, Federal Republic of Germany

The properties of the Omega sensor for stress measurements in textile and other flexible materials have been investigated under static and dynamic conditions. During free-flight tests with circular flat parachute models, the sensor was used to measure simultaneously the radial and circumferential stresses in adjacent gores. For comparison, the tensile force at the confluence point was also sensed by means of a force transducer. The time histories of the radial stress and the tensile force were similar. The maximal radial stress was about four times larger than the maximal circumferential stress.

I. Introduction

THE measurement of stress in the flexible material of deploying parachute canopies has been a research objective of the Institut für Flugmechanik for a long time. The main problem was that the known sensors either provided only the maximal stress value or caused such large local disturbances and interference that the recorded stress time histories were useless. Recently, Heinrich and Noreen[1] successfully solved the problem by designing a sensor shaped like the capital Greek letter omega (Figs. 1 and 2). This shape provides the required flexibility. When stress is applied to the tabs of the sensor, its curved beam is deflected and the resulting bending moment is measured by an active 120-ohm strain gage (Fig. 3). A second passive strain gage is added for temperature compensation. When the sensor is glued onto the textile, a small slit in the textile just under the slot of the sensor reduces the interference problem. The sensor had been tested for its static and dynamic properties and it was found to work satisfactorily.[2-4]

In 1974 an initial test series with the Omega sensor was prepared in the Institut für Flugmechanik's free-flight test facility.[5-7] The sensor was mounted on circular flat parachute models (nominal diameter $D_0 = 1.07$ m), which were then launched horizontally from a cannon operating on compressed air.

The results were both satisfactory and unsatisfactory. In most cases, the delicate sensors survived the rough mechanical loads applied during the packing and deployment of the parachutes. However, as was later detected, even though shielded leads had been used, the output signals were extremely disturbed by the high-frequency transmissions from a nearby AM broadcasting station and the test vehicle's FM telemetry transmitter.

Since the results looked promising enough, a thorough investigaton of the Omega sensor was carried out,[8] including qualification tests, the necessary improvement of the

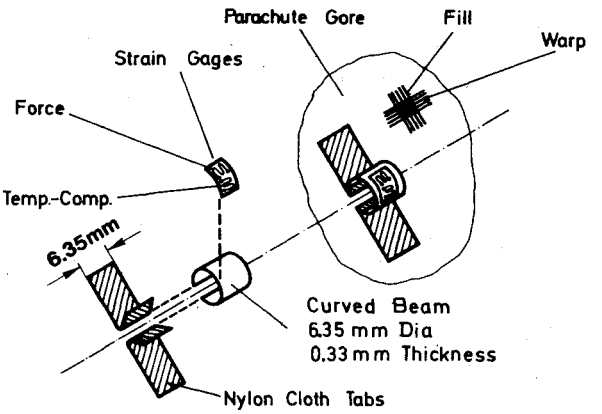

Fig. 1 Principle of Omega sensor.

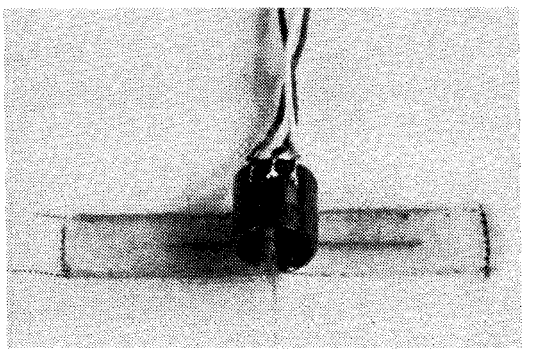

Fig. 2 Omega sensor mounted on textile.

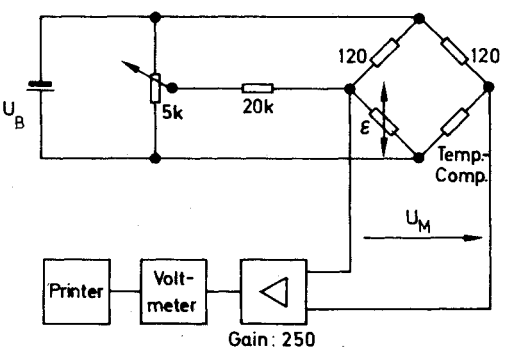

Fig. 3 Wiring diagram for sensor tests.

Presented as Paper 79-0435 at the AIAA 6th Aerodynamic Decelerator and Balloon Technology Conference, March 5-7, 1979; submitted July 23, 1979; revision received Dec. 28, 1979.

Index categories: Deceleration Systems; Testing, Flight and Ground; Sensor Systems.

*Section Leader, Digital Systems, Flight Test Engineering Division.

†Head, Applied Mathematics and Data Handling Division, Member AIAA.

Table 1 Test program with Omega sensors

No.	Static test	Dynamic test	Parameter tested	Sensor: Without textile	Sensor: With textile	Textile: Without slit	Textile: With slit	Test equipment	See Fig.
					Width, b (mm)		Length, b_{sl} (mm)		
1	X		Deflection	X				Micrometer sledge	4
2	X		Force (stress)	X				Static force balance	5
3	X		Temperature	X				Static force balance and temperature chamber	6
4		X	Vibration (eigenfrequencies)	X				Vibration test setup	7
5	X		Width of specimen		200-6.4	X			8 and 9
6	X		Width of specimen		200-6.4		6.4	Textile test machine	10
7	X		Length of slit		200		0-12		11
8		X	Rate of strain		200-6.4		6.4	MTS machine	12
9	Free-flight tests		Stress		X		6.4	Free-flight test facility	13-20

Table 2 Omega sensor specification data

Materials and Dimensions	
Curved beam	Stainless Steel Diameter = 6.35 mm Width = 6.35 mm Thickness = 0.33 mm
Tabs	Nylon, MIL-T-5608 E, Class A, Type I, width = 6.35 mm
Strain gages	SR-4, type FEAT-06B-12S9, foil gage, 120 ± 0.2Ω (BLH Electronics)
Adhesive for tabs and strain gages	Z 70 (HBM Hottinger Baldwin Meβtechnik)
Characteristics	
Sensitivity	Linear 2.94 ± 2% mV/(N/mm), at $U_B = 3$V
Thermal zero shift	−0.016 V/°C at $U_B = 5$V
Thermal sensitivity shift	Insignificant
Maximum stress loading	1.2N/mm
Supply voltage	$U_B = 3$ V

equipment for free-flight tests, and several free flights with parachute models. In this paper, typical results of the test program (Table 1) are reported.

II. Sensor Qualification Tests

Sensor without Textile

The sensors were manufactured in the Institute's laboratory. Some specifications are given in Table 2. To insure that these sensors would work acceptably well, it was necessary to run static and dynamic tests before they could be used for meaningful stress measurements.

First, the influence of deflection, force (stress), temperature, and vibration (eigenfrequencies) on the sensor without textile was measured.

Deflection

The tips of the nylon tabs were deflected a distance s. The output signal of the Omega sensor (Fig. 4) was nonlinear and showed some hysteresis due to creeping of the nylon material.

Force (Stress)

The sensor was loaded with weights up to 5 N. In Fig. 5, the static calibration curves of four sensors are plotted. The sensors have linear response to static force and, therefore, to static stress. The stress σ was computed by dividing the weight F by the width of the nylon tabs b_0.

Temperature

At three different stress levels the ambient temperature was changed. The output signals were registered after equilibrium had been achieved (Fig. 6). The slope $dU_{out}/d\sigma$ stayed constant, but a zero shift occurred. The stress characteristic of the sensor remained linear. The sensor indicated increasing stress with decreasing temperature because the strain gage was mounted on the concave side of the curved beam, which extends when the beam is heated but contracts when the beam is bent by a tensile force.

Since, like every electrically powered system, the sensor is itself a heat source, it will warm up when stored in a container with a parachute and then cool down after the release of the parachute. This can cause a very large error when the stress level is small; for example, during the steady descent of a parachute-load system. To reduce the temperature effects, the input voltage U_B was changed from 5 to 3 V.

Vibration (Eigenfrequencies)

For any application of the sensor, its eigenfrequencies are of particular interest. The sensor without nylon tabs was glued to a heavy steel plate (Fig. 7), which could be vibrated. The deflections of a light beam, reflected by a mirror attached to the sensor, showed resonance at 1.79 and 3.45 kHz. During earlier wind-tunnel measurements of parachute models nearly similar in size,[9] the model eigenfrequencies due to buffetting were about an order-of-magnitude smaller. Therefore, it was assumed that the Omega sensor would not show severe resonance effects.

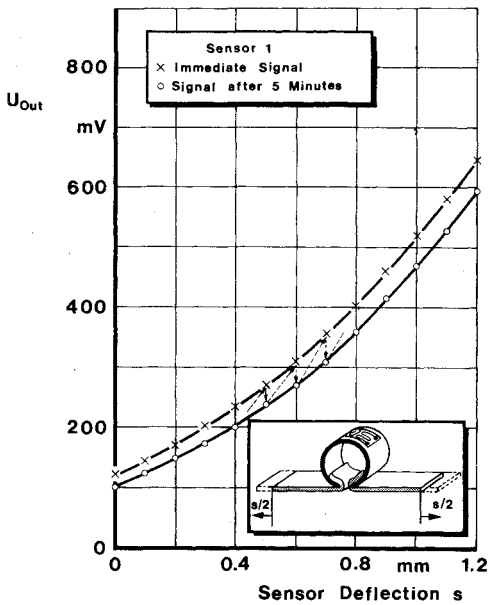

Fig. 4 Influence of nylon tabs during deflection; $U_B = 5V$, gain = 250.

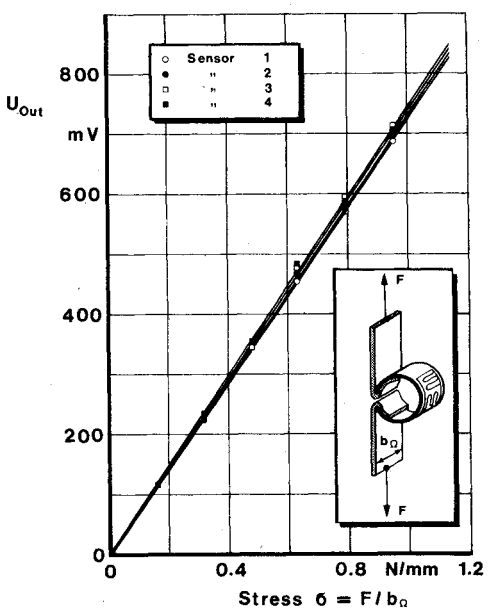

Fig. 5 Static calibration curves of four Omega sensors; $U_B = 3V$, gain = 250.

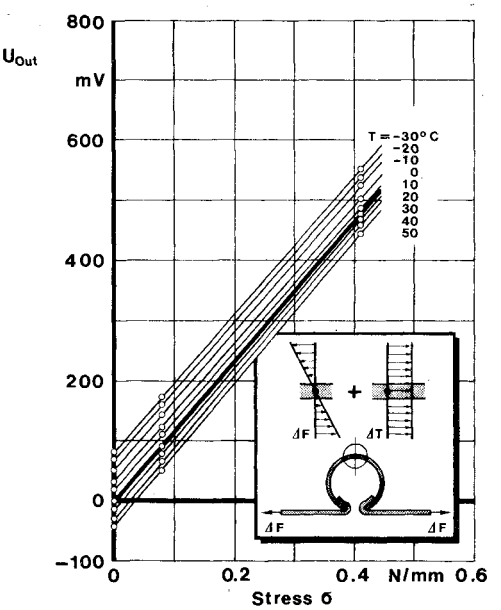

Fig. 6 Temperature sensitivity; $U_B = 5V$, gain = 250.

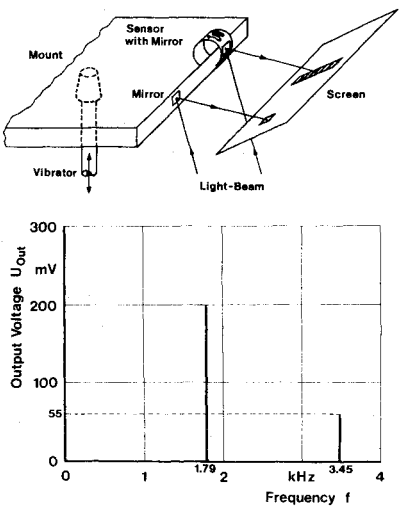

Fig. 7 Eigenfrequencies; $U_B = 3V$, gain = 250.

Sensor Mounted on Textile Specimen

The next step was to investigate the combined system of the Omega sensor with textile. For the sensor to function on parachutes, the influence of the geometry of the textile on the measurement should be tolerably small. To ascertain this, the sensor was mounted on a textile specimen of varying width b (Figs. 8-10). Stress was applied in a textile machine. In Fig. 9 one can see the importance of the slit in the textile below the sensor; without slit the fraction of the load carried through the sensor varied with the width of the specimen. But, as soon as a slit was made, the sensor signal became reasonably independent of the specimen. When the length of the slit was made equal to the width of the sensor, $b_{sl} = b_\Omega = 6.4$ mm, all sensor signals fell within the shaded region in Fig. 9, which lies around the static calibration curve of the sensor without textile. As Fig. 10 shows in detail, the slopes of the sensor signals with and without textile became nearly equal. This means that the sensor can be calibrated before being attached to the textile. The scattering of the sensor signals around the static calibration curve was within the limits -35 mV $< \Delta U_{out} < 120$ mV. This corresponds to an absolute error of -0.05 N/mm $< \Delta\sigma < 0.17$ N/mm and a relative error of $-4\% < \Delta\sigma_{rel} < 14\%$ related to the maximum stress loading ($= 1.2$ N/mm).

There are two effects contributing mostly to these deviations:

1) The sensor signal is very sensitive to the length of the slit (see Fig. 11). Therefore, the slit was made by cutting a specific number of threads per millimeter under a microscope. The slit was checked carefully during the tests.

2) Due to creeping of the textile under load, the sensor was carrying a bigger share of the load when the applied load was decreasing. Thus, for decreasing stress the indicated stress was too large.

For completeness, the influence of the rate of strain, $d\epsilon/dt$, was tested (see Fig. 12). Up to $d\epsilon/dt = 500\%/s$, the influence remained insignificant.

The conclusion from the results of the laboratory tests was that the Omega sensor can be used to measure stress in flexible materials. The next step, therefore, was to carry out experiments with the Omega sensor under free-flight conditions.

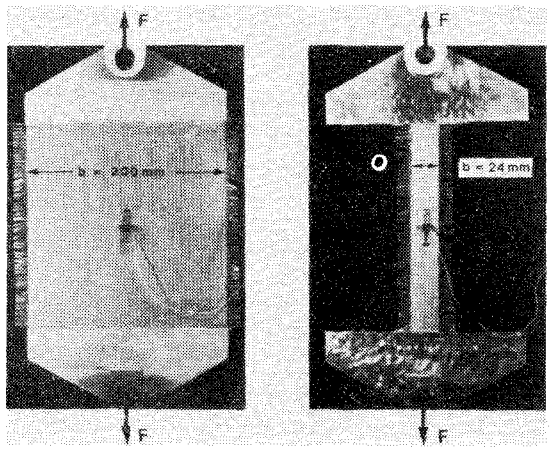

Fig. 8 Textile specimen with Omega sensor; $\sigma = F/b$.

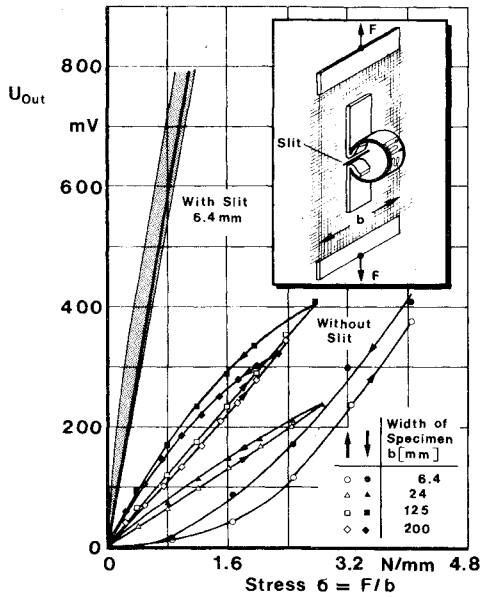

Fig. 9 Sensor signal vs average stress σ for different widths b of textile specimen with and without slit; $U_B = 3$V, gain = 250.

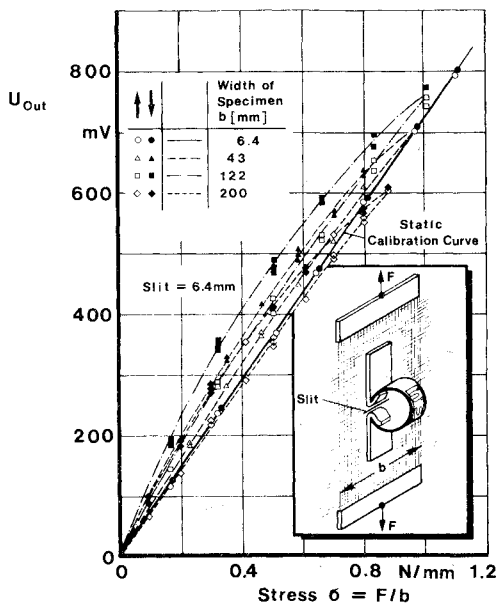

Fig. 10 Sensor signal vs average stress σ for different widths b of textile specimen with slit $b_{sl} = 6.4$ mm; $U_B = 3$V, gain = 250.

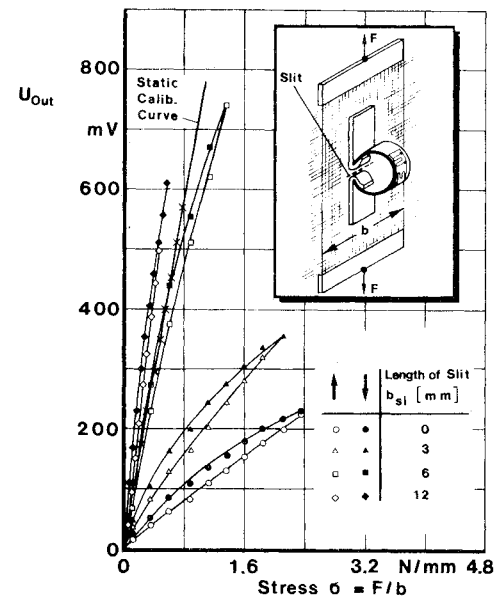

Fig. 11 Sensor signal vs average stress σ for different lengths b_{sl} of slit; $b = 200$ mm, $U_B = 3$V, gain = 250.

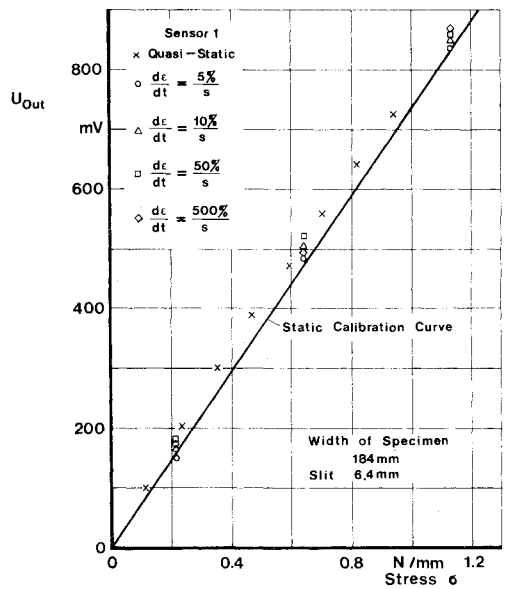

Fig. 12 Influence of the rate of strain; $U_B = 3$V, gain = 250.

III. Stress Measurements on Parachutes During Free Flight

Free-Flight Test Facility

The DFVLR-Institut für Flugmechanik has a test facility for the horizontal launching of masses 2-30 kg at corresponding maximum speeds of between 250 to 70 m/s (Fig. 13). For tests with parachute models, a number of vehicles 110 mm in diameter were developed (Fig. 14). The vehicles have different sections for the conical antenna and the power pack, the FM telemetry (6-channel) transmitter with several amplifiers, the force transducer, and the test parachute.

Stress Measurements

The Omega sensors were mounted along the centerline of the gores of circular flat parachute models (nominal diameter $D_0 = 1.07$ m) (Fig. 15). The distance from the hem was 50 mm. To eliminate the high-frequency telemetry disturbances which had been observed during earlier tests, special amplifiers were developed for the stress measurement. These amplifiers were attached to a suspension line close to the Omega sensor. Figure 16 shows the block diagram for the free-flight tests.

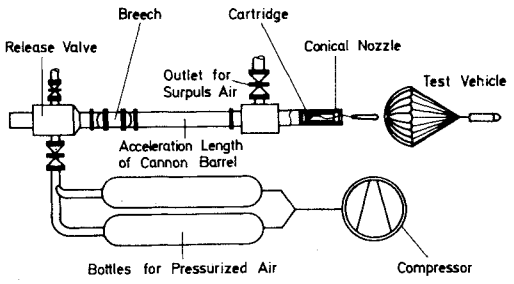

Fig. 13 Free-flight test facility.

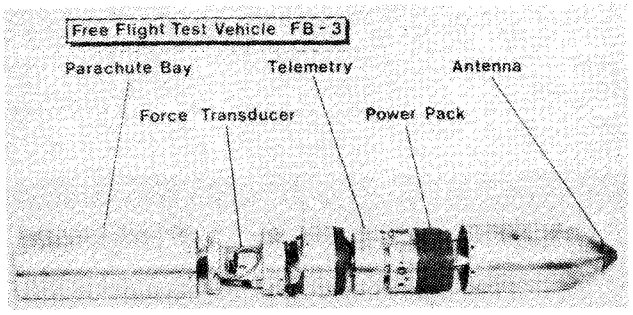

Fig. 14 Test vehicle for parachutes.

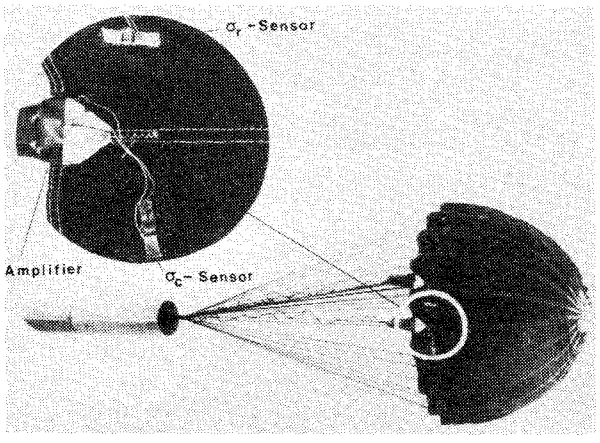

Fig. 15 Parachute model with Omega sensors; circular flat canopy, $D_0 = 1.07$ m (3.5 ft), 28 gores, length of suspension lines $l_s = 0.97$ m.

Two test series, each of ten flights, were carried out. At first only one sensor was used to measure the circumferential stress and to learn how to handle the delicate sensor. Then, during the second test series, a second sensor was mounted on the adjacent canopy gore, with its active direction perpendicular to the first sensor to measure the radial component of the stress. In all cases the initial speed V_0 of the vehicle was about 70 m/s.

Figure 17 shows the analog paper recordings of two flights. The time histories of the total suspension line force, the circumferential stress, and the radial stress are recorded. In addition, the pulses of two photocells, t_1 and t_2, were registered for computation of the initial speed V_0. The time scale is 0.1 s.

At initial time t_0, the parachute load system was accelerated up to 100 g. The Omega sensors, stored with the parachute in the vehicle, were compressed somewhat by the parachute mass. Accordingly, their signals deviated from the static zero outputs. After 0.15 s, the test vehicle left the barrel of the air cannon and passed both photocells which were 0.5 m apart. The parachute was then deployed by a static line. In the interval between deployment and line stretch, both Omega

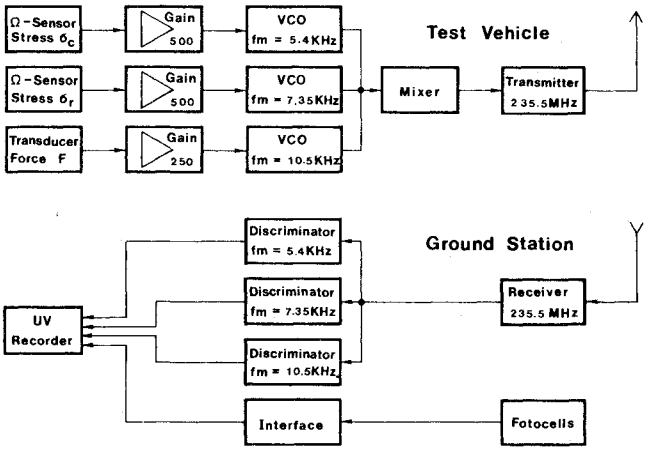

Fig. 16 Block diagram for free-flight tests.

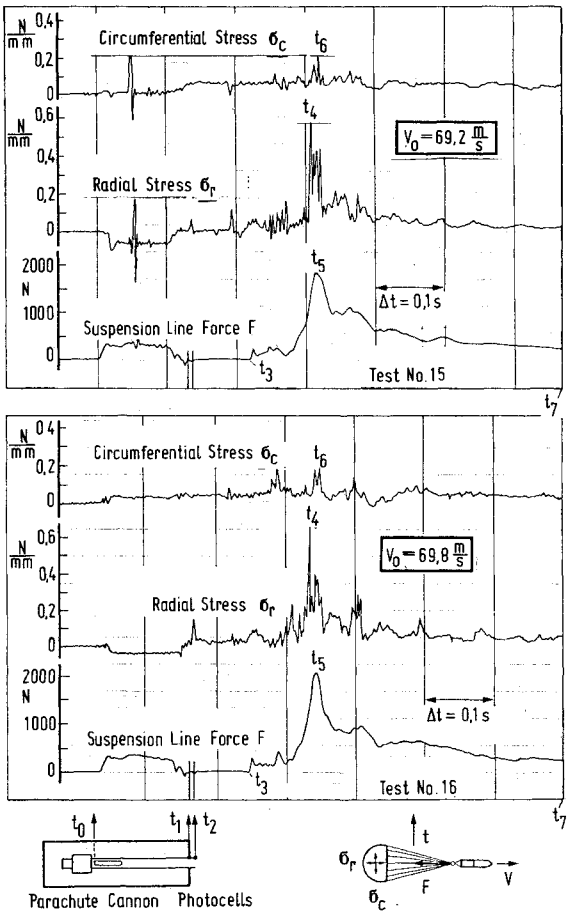

Fig. 17 Recorded stress and force time histories from free-flight tests with circular flat parachute models.

sensors experienced some external forces from contact with the parachute's materials.

After the suspension lines were stretched, both stress sensors recorded positive oscillating stress loads. This indicates fluttering of the canopy material.

When the maximum filling force, the filling shock F_f, occurred, the stress signals also reached their maxima. Since the force signal was recorded at the confluence point of the suspension lines, there had to be a time lag between the force and the stress signal. This explains why the radial stress maximum occurred about 10 ms before the filling shock. The radial stress signal was quite similar to the force signal, but

with superimposed vibrations of higher frequencies. The maximal radial stress was about four times larger than the maximal circumferential stress.

Normalized Stresses

At initial speeds of $V_0 = 70$ m/s, the vehicle's free-flight time was about 0.5 s from leaving the nozzle of the cannon to hitting a curtain of vertical belts at the end of the test section. Doubtless the vehicle was not slowed down to the steady-state speed; however, the filling of the parachute was completed, as the force signal in Fig. 17 shows, and the parachute was fully open. At $t = t_7$, the average force and the average stresses may be assumed to be proportional to the dynamic pressure alone. Then the normalized stress should become equal to the normalized steady-state stress

$$\sigma^*(t_7) = \sigma^*(t \to \infty) = \sigma^*_{ss}$$

and, by the same argument,

$$C_{D0}(t_7) = C_{D0}(t \to \infty) = C_{D0}$$

Therefore, the dynamic pressure can be determined from

$$q(t_7) = F(t_7)/C_{D0}S_0$$

Taking $C_{D0} = 0.7$, the dynamic pressure at the end of the free flight is

$$q(t_7) \approx 350\ \text{N/m}^2 \approx 7\ \text{lb/ft}^2$$

To evaluate

$$q(t) = \rho/2V(t)^2$$

the suspension line force was integrated, giving

$$V(t) = V_0 + \frac{k}{m_1}\int_{t_2}^{t} F(\tau)\,d\tau$$

(see Fig. 18); $m_1 = 5$ kg is the vehicle's mass. The vehicle's drag was neglected. To compensate for this and similar errors, such as nonlinearities in the calibration curves, the factor k was introduced; k was determined using the known boundary condition $q(t_7)$.

In Table 3, the normalized stresses σ^* are presented for different times.

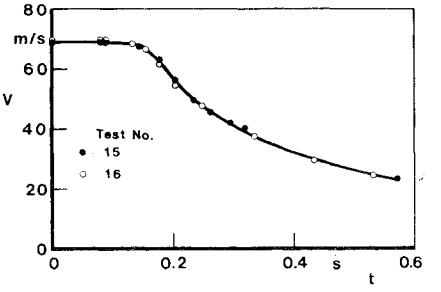

Fig. 18 Vehicle speed vs time.

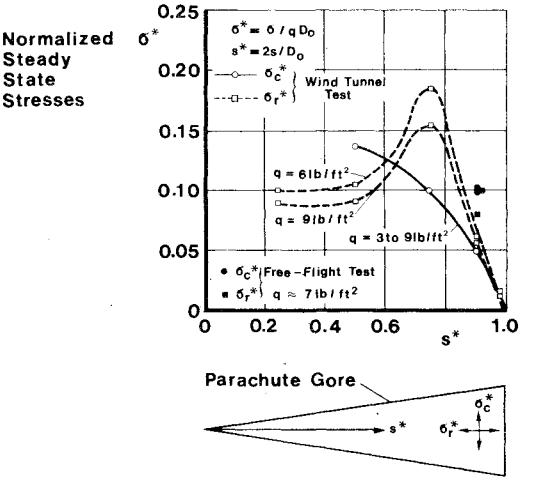

Fig. 19 Comparison of normalized circumferential stress $\sigma^*_r(t=t_7)$ and normalized radial stress $\sigma^*_r(t=t_7)$ with steady-state wind-tunnel measurements by Heinrich and Saari.[10]

Steady-State Stresses

$\sigma^*_r(t_7)$ and $\sigma^*_c(t_7)$ were plotted in Fig. 19 together with normalized steady-state stresses from wind-tunnel measurements (see Fig. 5).[10] Since at the end of the free flight the registered signals were already small, the $\sigma^*_r(t_7)$ and $\sigma^*_c(t_7)$ values were uncertain. Considering this, the comparison with the wind-tunnel data shows reasonable agreement.

Maximal Stresses

During all free-flight tests with this parachute model, the normalized maximal circumferential stress σ^*_{mc} was much less

Table 3 Data from free-flight Tests Nos. 15 and 16

		Test No. 15						Test No. 16					
		Start of free flight t_2	Line stretch t_3	Max, σ_r σ_{mr} t_4	Max, F F_f t_5	Max, σ_c σ_{mc} t_6	End of free flight t_7	Start of free flight t_2	Line stretch t_3	Max, σ_r σ_{mr} t_4	Max, F F_f t_5	Max, σ_c σ_{mc} t_6	End of free flight t_7
t	s	0	0.083	0.174	0.177	0.187	0.57	0	0.079	0.169	0.175	0.187	0.530
v	m/s	69.2	69.2	62.2	62.0	60.0	23.7	69.8	69.8	61.7	61.3	60.0	24.6
q	N/m²	2930	2930	2368	2355	2203	345	2982	2982	2330	2300	2203	372
F	N	0	0	1300	1608	1541	217	0	0	1263	1787	1216	234
σ_r	N/mm	0.042	0.049	0.563	0.424	0.424	0.031	0.146	0.042	0.612	0.375	0.375	0.042
σ_c	N/mm	0.054	0.054	0.047	0.134	0.190	0.040	0.040	0.040	0.080	0.170	0.172	0.040
$F/qC_{D0}S_0$		0	0	0.87	1.09	1.11	1.00	0	0	0.86	1.24	0.88	0.100
$\sigma^*_r = \sigma_r/qD_0$		0.013	0.016	0.222	0.168	0.180	0.084	0.046	0.013	0.245	0.152	0.159	0.106
$\sigma^*_k = \sigma_c/qD_0$		0.017	0.017	0.019	0.053	0.081	0.108	0.013	0.013	0.032	0.069	0.073	0.100
				0.956						0.929			

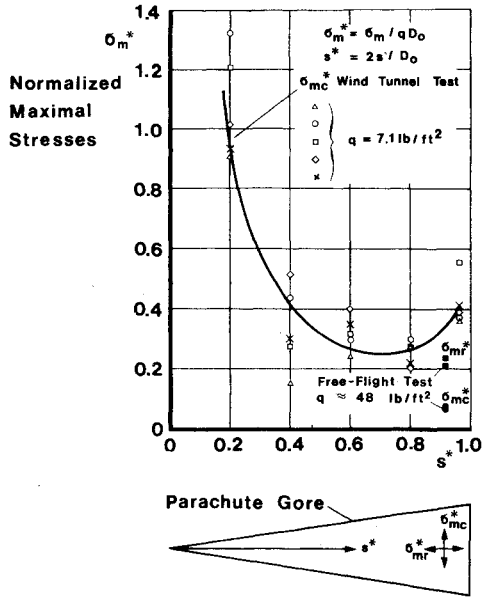

Fig. 20 Comparison of normalized maximal circumferential and radial stresses, σ_{mc}^* and σ_{mr}^*, with wind-tunnel measurements by Heinrich and Saari.[10]

than the normalized maximal radial stress σ_{mr}^*. The comparison in Fig. 20 of σ_{mc}^* with wind-tunnel results from Fig. 10 of Ref. 10 shows that σ_{mc}^* was also much less than the corresponding wind-tunnel data. The free-flight data should be somewhat smaller due to the finite mass effect. But, during free flight, the mass number was fairly high at $\mu = m/\rho D_0^3 \approx 3.6$. Therefore, the finite mass effect should not have been significant.

From Fig. 5 of Ref. 10, it follows (see Fig. 19) that the ratio σ_r^*/σ_c^* varies with the position on the gore. It may be that the shapes of the gores of the free-flight model and the wind-tunnel models were slightly different due to different production techniques, so that our model experienced less maximal circumferential stress near the canopy skirt.

IV. Conclusions

The results obtained by the static and dynamic tests with the Omega sensor confirmed that this sensor can be used to measure stress in the material of flexible parachute canopies. During free-flight tests with circular flat parachute models, it was possible to record the radial and circumferential stresses near the canopy skirt.

The next steps of the research program should be to improve the sensor by reducing its temperature sensitivity and to carry out more free-flight tests in order to study the stress distribution over the gore geometry.

Acknowledgments

This research has been sponsored in part by the U.S. Air Force, Office of Scientific Research, Bolling AFB, Washington, D.C., and the European Office of Aerospace Research and Development, London.

Along with the staff of the Institut für Flugmechanik, R. Freese, a graduate student at the Technische Universität Braunschweig, participated in the research work and contributed considerably to the results. H.G. Heinrich from the University of Minnesota advised the Institute during the preparation of the initial tests.

References

[1] Heinrich, H. G. and Noreen, R. A., "Stress Measurements on Inflated Model Parachutes," AFFDL-TR-72-43, Dec. 1972.

[2] Heinrich, H. G. and Noreen, R. A., "Functioning of the Omega Sensor on Textile Samples under High Loading Rates," University of Minnesota, Final Rept., July 1973-May 1974, Contract F33615-73-C-3149, Sept. 1974.

[3] Braun, G., "Untersuchungen an einem Aufnehmer zur Messung von Spannungen in Fallschirmgeweben (Ω-Aufnehmer)," DFVLR-Institut für Flugmechanik, Braunschweig, Interner Bericht IB 154-77/30, Oct. 1977.

[4] Freese, R., "Untersuchungen an einem Aufnehmer zur Messung von Spanungen in Textilien," Studienarbeit, Institut für Grundlagen der Elektrotechnik und elektrische Meβtechnik, Technische Universität Braunschweig, Prof. Dr.-Ing. H.H. Emschermann, Dec. 1977.

[5] Braun, G., "Druckbeschleunigungsanlage für Modellfallschirme," DFVLR-Institut für Flugmechanik, Braunschweig, Interner Bericht IB 154-73/2, Feb. 1973.

[6] Klewe, H.-J., "Measuring Techniques in Rescue and Recovery Systems," AGARD-Cranfield-DFVLR Short Course, Flight Instrumentation, June 1977.

[7] Doherr, K.-F. and Hamel, P., "Beiträge der DFVLR zur Untersuchung von Rettungs- und Bergungssystemen," *Zeitschrift für Flugwissenschaften* (*ZfW*), Vol. 22, Nov. 1974, pp. 153-163.

[8] Braun, G. and Doherr, K.-F., "Experimentelle Untersuchung von Omega-Aufsnehmern zur Messung der Spannung in flexiblen Fallschirmkappen," DFVLR-Institut für Flugmechanik, Braunschweig, Interner Bericht IB 154-78/15, Aug. 1978.

[9] Doherr, K.-F., "Theoretical and Experimental Investigations of Parachute-Load-System Dynamic Stability," AIAA Paper 75-1397, AIAA 5th Aerodynamic Decelerator Systems Conference., Albuquerque, N.M., Nov. 1975.

[10] Heinrich, H. G. and Saari, D. P., "Parachute Stress Measurements at Steady State and During Inflation," *Journal of Aircraft*, Vol. 15, Aug. 1978, pp. 534-540.